IEEE Access
Multidisciplinary | Rapid Review | Open Access Journal

Received August 18, 2020, accepted September 7, 2020, date of publication September 18, 2020,
date of current version September 28, 2020.

Digital Object Identifier 10.1109/ACCESS.2020.3024534

Black-Box Small-Signal Structure for Single-Phase and Three-Phase Electric Vehicle Battery Chargers

ANTREAS NAZIRIS, (Student Member, IEEE), AIRAN FRANCES, (Member, IEEE), RAFAEL ASENSI, AND JAVIER UCEDA, (Life Fellow, IEEE)
Centro de Electrónica Industrial (CEI), Universidad Politécnica de Madrid, 28040 Madrid, Spain

Corresponding author: Airan Frances (airan.frances@upm.es)

This work was supported by the Spanish Ministry of Economy and Competitiveness through the Project Sistema de identificación automática de modelos no lineales en caja negra de convertidores electrónicos de potencia en micro-redes inteligentes de corriente continua (IDENMRED) under Grant DPI2016-78644-P.

ABSTRACT At present, it is safe to say that the future belongs to sustainable technologies. Electric vehicles are one of the most representative sustainable solutions for mobility. Some of the many advantages they offer are a clean operation, a profit gain from a possible power return to the grid in vehicle to grid applications, grid power support, etc. As it is expected, an increase in the production of electric cars, and other battery-based systems, lead to an increment in battery chargers. Therefore, energy distributors must deal with many different schemes in the grid and with the amount of energy demanded from a fleet of cars and other electric vehicles. This paper deals with the modeling of AC/DC battery chargers by identifying the transfer functions in any operating condition without knowing the specific details inside those chargers. This approach is called black-box modeling and the strategy is based on the information provided by the input and output variables of the charger. The research illustrates the flexibility of the model to work with single-phase and three-phase AC/DC chargers which are linked to on-board and off-board charging stations. An extensive set of tests is shown, verifying the accuracy of the proposed models in a wide variety of operating conditions.

INDEX TERMS AC-DC power converters, battery chargers, black-box models, electric vehicles, modeling, power system dynamics, single-phase electric power, system identification, three-phase electric power.

I. INTRODUCTION

Different kinds of Electric Vehicles (EV) already exist on the market, like EVs (100% electric), Plugin Hybrid EVs (PHEV), and Fuel Cell EVs (FCEV) [1], [2]. Also, the battery chargers of the EVs come in different structures. The well-distributed approach is unidirectional, where battery chargers can only take the energy from the grid to charge the battery. However, a big amount of EVs requesting power at the same time can cause a huge drain in the grid. In order to add flexibility, bidirectional battery chargers have been introduced permitting either to take energy from the Grid to the Vehicle (G2V) and the opposite, taking the energy from the Vehicle to the Grid (V2G).

Another strand about EVs is whether to choose an on-board charger or an off-board charger [3], [4]. The main difference between them is the battery charging time based on different power ranges. On-board chargers used to have lower power ranges due to constraints in weight and volume. Nevertheless, each part has well-established advantages and disadvantages.

Bidirectional battery chargers let EV users interact with the grid in a more flexible fashion. The energy exchange gives an opportunity to reduce the charging cost and to provide ancillary services such as load peak leveling [5]–[10]. This is obtained by feeding back to the grid some of the stored energy, during some specific periods, leading to an economic profit. Furthermore, the energy stored in the batteries can be used to support the grid providing voltage and frequency regulation services [11], [12]. EVs are gaining more and more supporters and the companies are looking for different types of EVs aiming for more efficient and cheaper chargers. A huge increment of the power demanded to the grid is expected as a result of the increase in the number of EVs, hence, it would be desirable to have models able to estimate the grid behavior in this new scenario.

The approach used in this work is based on the black-box models of battery chargers. The black-box approach can identify the behavior of a device (with limited insight

The associate editor coordinating the review of this manuscript and approving it for publication was Xiaosong Hu.

information of this component) by using the information provided by the accessible input and output variables, combined with identification methods, to create a behavioral model [13]. Black-box models can reduce the time-to-market of the installation, simplify the design of protections systems, and reduce the risk of destruction of components due to unexpected behaviors. In the literature, most of the black-box proposals for electronic power converters are dealing with DC/DC converters [14], [15]. Modeling approaches are grouped by the kind of behavior that the model is capable to reproduce. The most popular are the small-signal linear models. The process of obtaining the transfer functions in this approach can be implemented in time [16] and in the frequency domain [17], [18], with an accurate representation of the dynamic behavior around an operating point of any converter.

In the literature, only a few examples of black-box models for AC/DC or DC/AC can be found due to its complex construction. Most of the approaches use the d-q rotating framework to transform the AC signals in DC ones, so most of the techniques applied to DC/DC converters can be used. In [19] a method to identify the input and output impedances of three-phase voltage source converters is proposed, where the focus is on the stability analysis. In [20] and [21] the authors also consider DC/AC converters and the goal is to obtain a behavioral model extending the structures used for DC/DC converters. The former considers a voltage source inverter, whereas, the later deals with a grid-supporting inverter. Finally, it is possible to find also examples of AC/DC converters as [22], where the authors use frequency domain identification to obtain the black-box model of a simulated three-phase rectifier. Also [23] shows a black-box model of a rectifier, but for a radio-frequency application and the approach is completely different, based on a support vector regression machine.

In this context, the main contributions of this research are:

- To propose a black-box small-signal structure for the specific case of battery chargers, where both the input and output voltages are imposed.
- To include the effect of changes in the control references in the dynamic response of the output variables of the model.
- To propose a methodology to consider both single and three-phase AC signals in the modeling structure.

The paper is organised as follows. In Section II, a short review of black-box modeling techniques is included, describing the proposed small-signal black-box model structure. In Section III, the modeling strategy is applied to a detailed switching model of a battery charger, which is used as a reference. The results offered by the behavioral black-box model and the detailed switching model are compared through simulations. In Section IV, the black-box modeling strategy is applied to an actual battery charger, comparing the actual measurements and the results provided by the black-box model. Finally, in Section V some conclusions are provided, establishing the good behavior of the proposed model.

II. PROPOSED BlackBox MODEL FOR EV CHARGERS

The main purpose of this paper is to model accurately AC/DC converters with limited information about their internal design. In order to obtain such a model, the black-box approach will be applied. The idea behind the black-box modeling is the application of system identification techniques to obtain the converter transfer functions based on the information offered by the accessible input and output variables of the battery charger in a collection of tests.

The black-box modeling structure is well known in DC/DC converters [24]–[29]. To extend this modeling technique to AC/DC converters, the transformation of AC signals to DC signals through Park transformation is required. In general, the variables imposed to the system are set as input variables of the black-box model, whereas the remaining variables in the input and output ports are set as outputs of the model. Additionally, the control references of regulated converters can be included as additional inputs. In three-phase AC/DC battery chargers, typically, the variables imposed to the systems are the input and output voltages and the control references. In this case, it will be considered that the battery charger controls the battery current and the reactive power exchange with the grid, which can be used to provide reactive power support.

Consequently, the three-phase AC voltages (V_{abc}), the battery voltage, the charging current reference (I_{ref}), and the reactive power reference (Q_{ref}) are set as input variables in the model; whereas, the battery current (I_{bat}) and the three-phase AC input currents (I_{abc}) are set as output variables in the model. However, the battery voltage can be considered constant in the time scale of interest (the order to milliseconds), so it can be neglected in the small-signal model.

The three-phase voltages and currents can be transformed in DC variables in the d-q rotating axis through the Park transformation as indicated in Fig. 1 (a). Then, the new model has only DC variables, V_d, V_q, I_{ref}, and Q_{ref} as inputs and I_{bat}, I_d, and I_q as outputs. This model structure with DC input and output variables will be used throughout the paper.

In single-phase AC/DC converters an artificial Park transformation is applied, assuming the input voltage as V_α in the $\alpha\beta$ plane, generating V_β by a 90° phase shift of V_α and then making the transformation from the $\alpha\beta$ axis to the rotating d-q axis, as depicted in Fig. 1 (b). Through this transformation, both the single-phase and the three-phase d-q black-box models show a similar structure [30], [31].

If the small-signal conditions are met around an operating point, then the system could be considered linear, and the small-signal black-box model is easier to be obtained. Applying a small-signal step perturbation in one of the input variables and observing the perturbation in the output variables, a collection of transfer functions are easily obtained through identification algorithms. Doing the same with all the input variables, it can be obtained a number of transfer

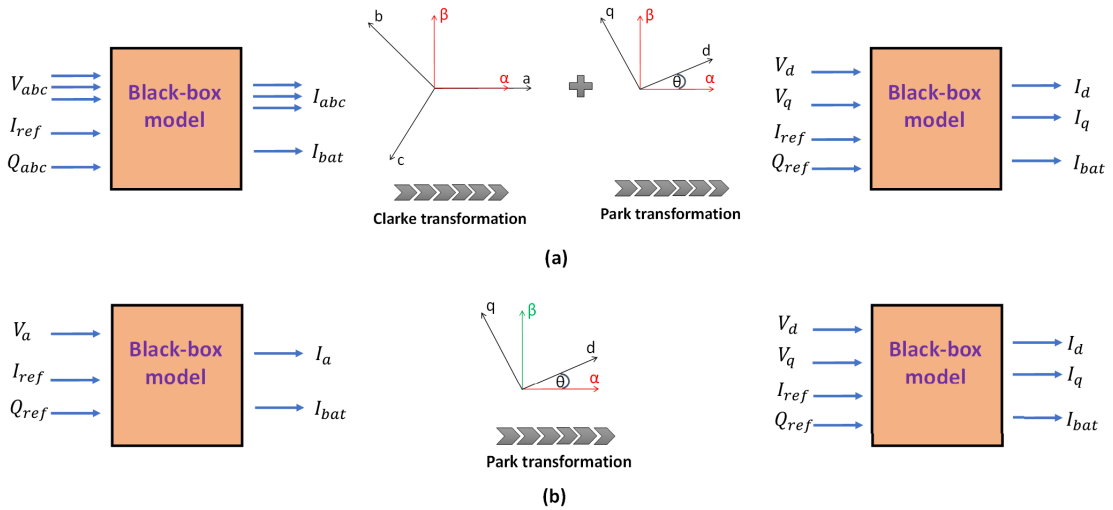

FIGURE 1. Battery charger transformation to D-Q framework: a) 3-ph AC/DC battery charger transformation to D-Q framework; b) 1-ph AC/DC battery charger transformation to D-Q framework.

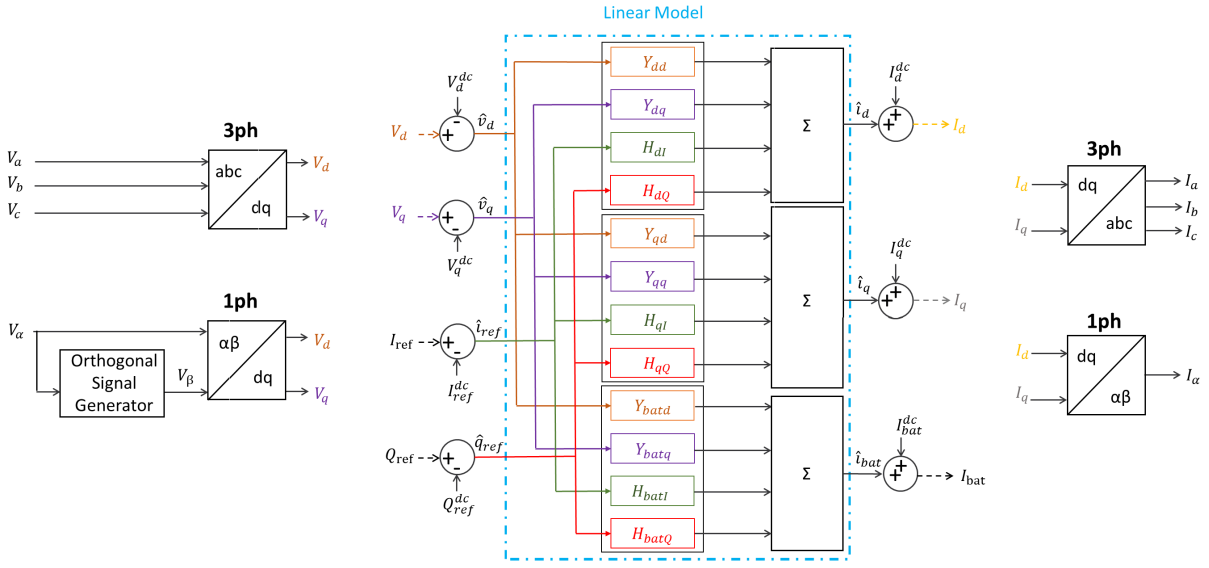

FIGURE 2. Block diagram of the black-box model.

functions equal to the number of output variables multiplied by the number of input variables. As linearity is assumed, the superposition theorem can be applied, and the small-signal model structure is represented in Fig. 2. Please note that, in that figure the variables are perturbations of the input and output variables around the operating point, and they are represented by $\hat{x}$ letters.

This block diagram of the small-signal model can be also represented by the following matrix equation (1):

$$\begin{pmatrix} \hat{i}_d(s) \\ \hat{i}_q(s) \\ \hat{i}_{bat}(s) \end{pmatrix} = \begin{pmatrix} Y_{dd}(s) & Y_{dq}(s) & H_{dI}(s) & H_{dQ}(s) \\ Y_{qd}(s) & Y_{qq}(s) & H_{qI}(s) & H_{qQ}(s) \\ Y_{batd}(s) & Y_{batq}(s) & H_{batI}(s) & H_{batQ}(s) \end{pmatrix} \times \begin{pmatrix} \hat{v}_d(s) \\ \hat{v}_q(s) \\ \hat{i}_{ref}(s) \\ \hat{q}_{ref}(s) \end{pmatrix} \quad (1)$$

where, $Y_{dd}(s)$, $Y_{dq}(s)$, $Y_{qd}(s)$, $Y_{qq}(s)$, $Y_{batd}(s)$, $Y_{batq}(s)$, $H_{dI}(s)$, $H_{qI}(s)$, $H_{batI}(s)$, $H_{dQ}(s)$, $H_{qQ}(s)$, and $H_{batQ}(s)$ are the transfer functions that describe the dynamic response of the system, where the first subindex refers to the output and the second subindex refers to the input variable involved. For instance, $Y_{dq}(s)$ is the transfer function that describes the dynamic response of the d-component of the input current when the q-component of the input voltage is perturbed and the rest of the input variables are kept constant. The mathematical description of this transfer function can be expressed as follows:

$$Y_{dq}(s) = \left.\frac{\hat{i}_d(s)}{\hat{v}_q(s)}\right|_{\hat{v}_d(s)=0, \hat{i}_{ref}(s)=0}. \quad (2)$$

The rest of the transfer functions can be defined analogously. The small-signal model defined in (1) can be represented by the equivalent circuit depicted in Fig. 3.

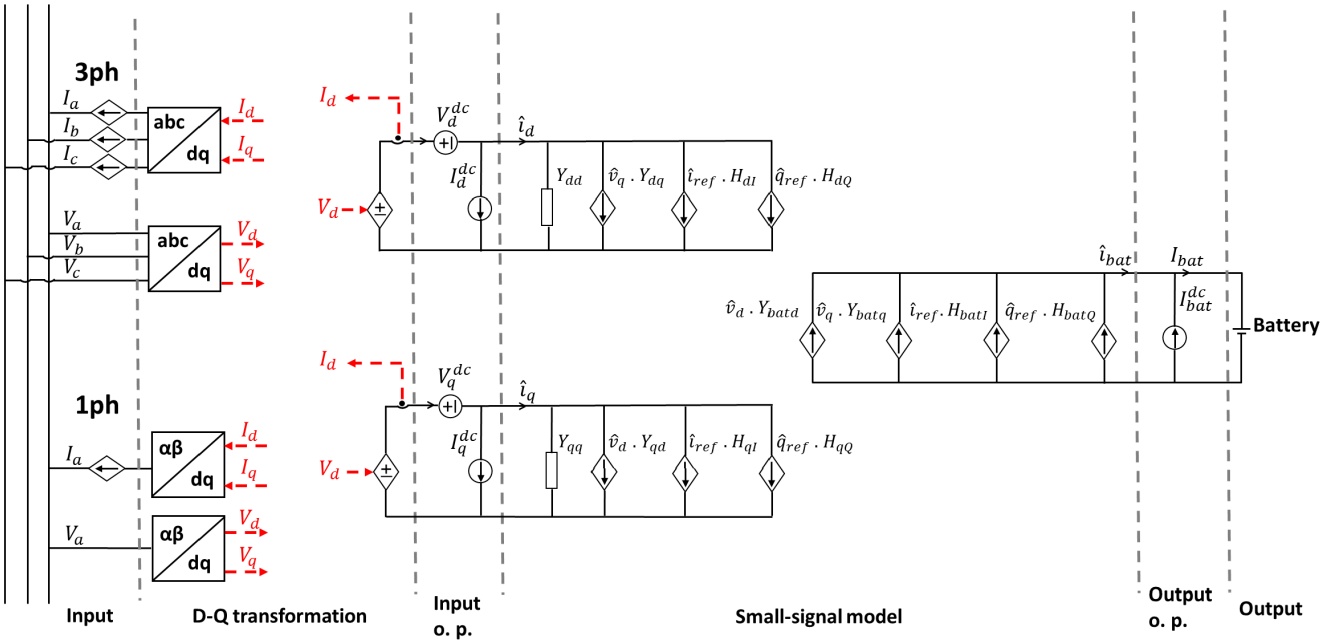

FIGURE 3. Equivalent circuit of the black-box model.

The limitations of this model come from the definition of small-signal average models and the use of the D-Q synchronous reference frame. Therefore, this model is useful for systems with a linear response or nonlinear systems around a specific operating point, which is considered as a dc bias in the model. On the other hand, it does not consider the switching ripple but it provides information about the average dynamic performance of the system. The synchronous reference frame restrains the model to balanced conditions of the grid and it only provides useful information about its fundamental frequency. Consequently, this paper provides information, through simulations and experimental results, about the usefulness of the model to describe the dynamic response of battery chargers.

A. MODELING PROCEDURE

The procedure to obtain the model is as follows. First, an operating point is selected, defined by the values of the inputs and outputs variables in steady state. Then, associated to this operating point, a small-signal model is generated. This small-signal model is characterized by twelve transfer functions as in the block diagram of Fig. 2. To obtain these twelve functions, small-signal steps around the operating point values are applied to every input, one by one, observing the perturbation in the output variables, while the rest of the input variables are kept constant. With this information by means of identification algorithms in MATLAB, the transfer functions represented in the block diagram of Fig. 2 are generated. The small-signal model can be also represented by the equivalent circuit of Fig. 3. The order of the transfer functions identified should be the lowest value that provides the highest degree of accuracy. The order selection often becomes a trade-off between accuracy and complexity.

The model structure proposed has four inputs: v_d, v_q, I_{ref}, and Q_{ref}. Therefore, four tests are necessary to obtain the transfer functions that describe the system. The first test should perturb the d-component of the input AC voltage, while the q-component is kept constant, as well as the references of the battery current and reactive power. The input AC voltage in a balanced three-phase system can be defined as follows (3):

$$\begin{aligned} V_a &= V_p \cdot cos(2 \cdot \pi \cdot f_{grid} \cdot t + \theta) \\ V_b &= V_p \cdot cos(2 \cdot \pi \cdot f_{grid} \cdot t - \frac{2 \cdot \pi}{3} + \theta) \\ V_c &= V_p \cdot cos(2 \cdot \pi \cdot f_{grid} \cdot t + \frac{2 \cdot \pi}{3} + \theta), \end{aligned} \tag{3}$$

where V_a, V_b, and V_c are the phase voltages of the three-phase AC input port, V_p is the amplitude of the phase voltage, f_{grid} is the frequency of the three-phase AC input voltage, and θ is the angle between the rotating vector that defines the three-phase AC input voltage and the d-component of the rotating D-Q frame, as depicted in Fig. 4(a). In this context, the d and q-components of the input voltage can be defined as (4):

$$\begin{aligned} V_d &= V_p \cdot cos(\theta) \\ V_q &= V_p \cdot sin(\theta). \end{aligned} \tag{4}$$

In order to perform steps in the d-component keeping the q-components constant and vice versa, it is useful to define V_p and θ according to the desired values of V_d and V_q as

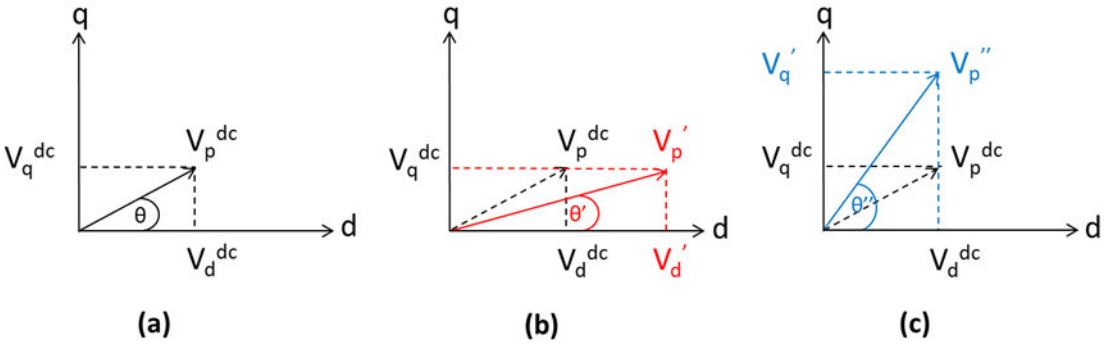

FIGURE 4. Three phase AC input voltage in the D-Q framework: (a) Operating point; (b) Step in the d-component; (c) Step in the q-component.

follows (5):

$$V_p = \frac{V_d}{cos\left(atan\left(\frac{V_q}{V_d}\right)\right)}$$
$$\theta = atan\left(\frac{V_q}{V_d}\right). \quad (5)$$

Therefore, due to the coupling between the d and q-components of the input voltage, it is necessary to change both the amplitude of the input voltage and its phase to make steps in each components without perturbing the other. In Fig. 4(b) it is depicted the V_p' and θ' necessary to generate a step V_d' without modifying V_q, whereas in Fig. 4(c) it is depicted the V_p'' and θ'' necessary to generate a step V_q' without modifying V_d.

In many cases, the use of a PLL (Phase-Locked Loop) makes V_q equal to zero. In those cases, V_d can be stepped by just making a step in V_p; and the input V_q and the transfer functions related to it ($Y_{dq}(s)$, $Y_{qq}(s)$, and $Y_{batq}(s)$) can be neglected. This simplification further reduces the number of transfer functions of the small-signal model to nine.

The third test should perturb the reference of the battery current (I_{ref}), while the d and q-components of the input AC voltage and the reference of the reactive power are kept constant. Similarly, the fourth test should perturb the reference of the reactive power (Q_{ref}), while the d and q-components of the input AC voltage and the reference of the battery current are kept constant.

Once all the transfer functions are completed, steady-state values of the output variables will be added to the perturbations to obtain the entire value of the output variables. The same procedure is used to create the perturbations on the input side of the model by subtracting the steady-state value of the input variable from the entire values of these variables, as depicted in Fig. 2 and Fig. 3.

III. SIMULATION RESULTS

In this section, the accuracy of the small-signal black-box model is verified through simulations. A single-phase bidirectional AC/DC converter is modeled in detail using the PSIM simulator, assuming this switching model is an accurate representation of the actual battery charger. Then, several tests are applied to the converter switching model using the simulator, following the procedure indicated in Section II-A. With the information provided by the input and the output variables, the transfer functions of the model are derived using MATLAB, and the black-box model is generated. Then, the responses of the black-box model and the switching model are compared in different conditions, showing a very similar dynamic behavior.

In Fig. 5, the schematic of the bidirectional battery charger is represented. It consists of an AC/DC boost rectifier, controlling the DC input voltage of the DC/DC converter and performing power factor correction. The rectifier is cascaded with a DC/DC Dual Active Bridge Converter, controlling the output current, which is followed by a battery. From this topology, a detailed switching model is generated using the PSIM simulator. Details about this model can be found in [32]. Using this model, it is possible to check the dynamic performance of the charger under different operating conditions and it is also used as a virtual equipment to be modeled using the black-box approach.

In Fig. 6, it can be observed the response of the AC input current (I_a) and the battery current (I_{bat}) when a step from 3 A to 9 A is given to the reference of the battery current (I_{ref}) at 0.05 s. The switching model in Fig. 6 is in orange colour and the black-box model in blue colour. Also, in yellow colour it has been included the AC voltage as reference of the phase of the AC current. As it is depicted in Fig. 2, the AC current of the black-box model comes from the combination of the small-signal response of both the d and q-components of I_a, plus the addition of their corresponding operating points, and finally the transformation from the D-Q framework to the $\alpha\beta$ plane. Therefore, the similarity between the switching model and the black-box model, both in amplitude and phase, demonstrates that the black-box model structure is adequate to reproduce the dynamic response of the input port of the battery charger when its control reference is perturbed. Similarly, Fig. 6 shows the comparison of the dynamic response of the controlled variable (output current) when its control reference is modified. This dynamic response includes the effect of the controller and the output filter of the converter, which is accurately reproduced by the black-box model.

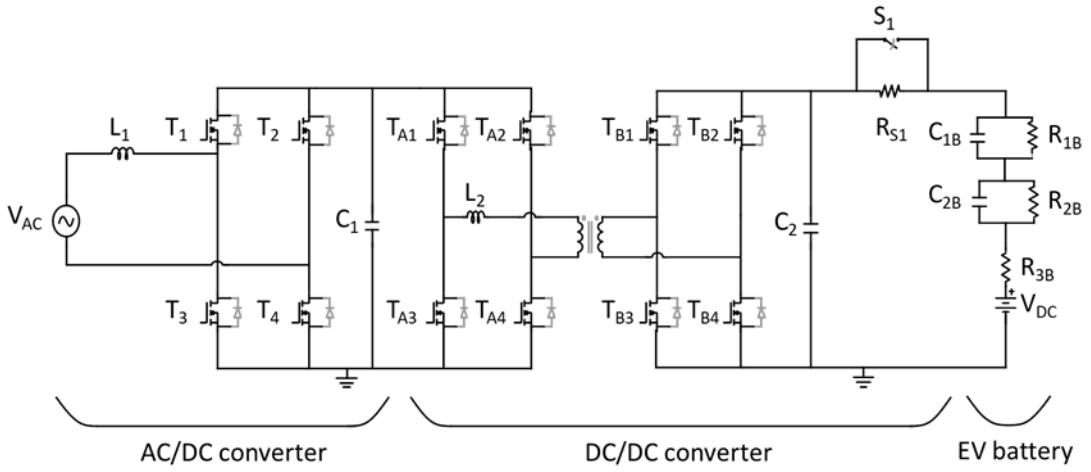

FIGURE 5. Schematic of the bidirectional battery charger.

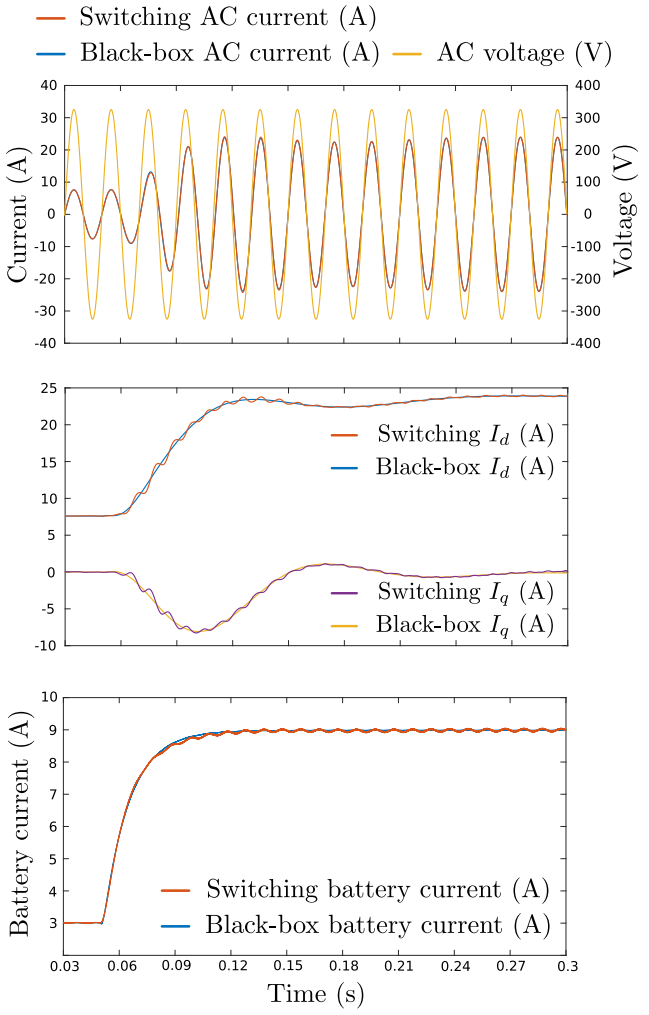

FIGURE 6. Comparison between the response of the switching model and the small-signal black-box model for a 6 A step in the reference of charging current in G2V operation: AC input current, D-Q input currents, and battery current.

In the second test, the reactive power control reference of the rectifier is perturbed. In this case, the reference is changed

TABLE 1. Identified transfer functions from the switching model.

TF	Identified TF
$H_{dI}(s)$	$\frac{-14s^2+4051+1.285e5}{s^3+59.9s^2+3605+4.7e4}$
$H_{qI}(s)$	$\frac{-0.155s^3+48.39s^2-6093s-3845}{s^3+71.57+4218s+9.977e4}$
$H_{batI}(s)$	$\frac{-30.46s+6.21e4}{s^2+927.4s+6.21e4}$
$H_{dQ}(s)$	$\frac{-0.1924s^2+1.6411s-3.519}{s^3+70.64s^2+4340s+69110}$
$H_{dQ}(s)$	$\frac{-0.1924s^2+1.6411s-3.519}{s^3+70.64s^2+4340s+69110}$
$H_{batQ}(s)$	*Neglected*

from 0 to 1000 *var* at 0.05 *s*. In Fig. 7 the response of the AC input current (I_a) of the switching model is compared with the black-box model. As the battery current remains constant, H_{batQ} is neglected. The switching model is included in orange colour, whereas the black-box model is presented in blue color. Also, the AC voltage has been included in yellow colour as reference for the phase of the AC current, which is especially relevant in this test. The control reference is the reactive power reference (Q_{ref}), which can be included in the model structure analogously to the case of the battery current reference (I_{ref}) in Fig. 2.

The approach to identify the model is the same: the AC current is decomposed in its d and q-components by means of an orthogonal signal generator, the transfer functions that

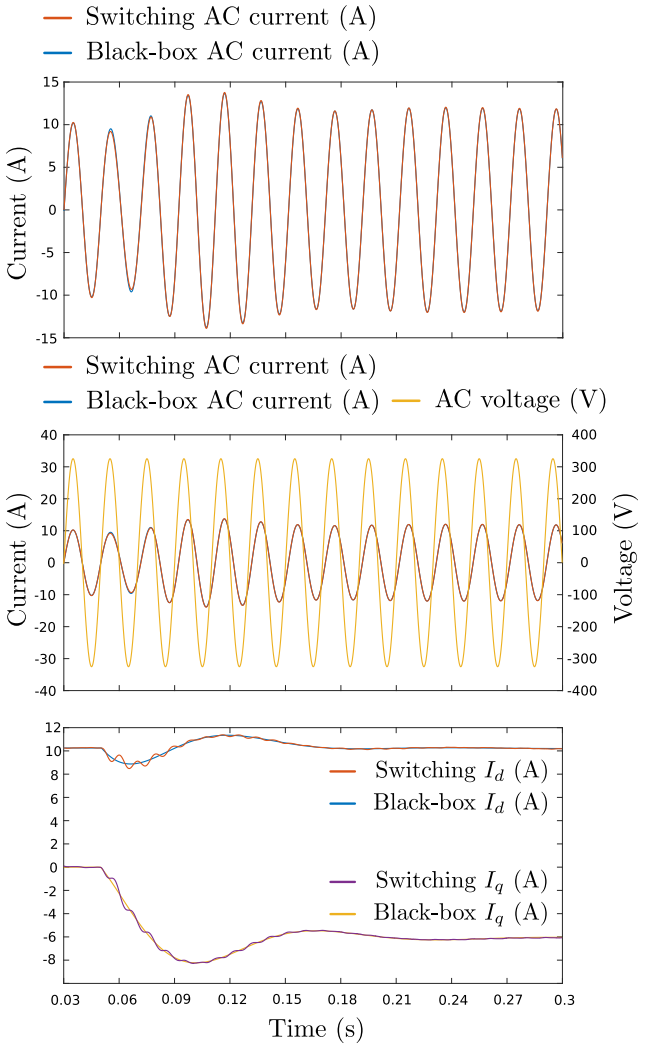

FIGURE 7. Comparison between the response of the switching model and the small-signal black-box model for a 1000 VAr step in the reference of reactive power: AC input current and D-Q input currents.

represents the dynamic response of these components are identified, and the AC signal is composed by adding the DC operating points to the response of the transfer functions and performing the transformation from the D-Q framework to the $\alpha\beta$ plane. It can be seen that this structure is able to reproduce with high accuracy the amplitude and phase of the single-phase AC current when a step in the reactive power reference is performed.

Consequently, the results shown in Fig. 6 and Fig. 7 demonstrate that the black-box model structure proposed for single-phase battery chargers is able to reproduce the dynamic response of their input and output ports when the control references are perturbed. The transfer functions identified for these experiments are included in Table 1.

IV. EXPERIMENTAL RESULTS

The experimental setup consists of a bidirectional AC/DC converter (Cinergia B2C-30), which is the main component of the setup and 2 E-BIKE Batteries (Electric Bicycle Bike Silverfish Li-Ion Battery). The details about the components included in the experimental setup are described in Table 2. In Fig. 8 the experimental setup is depicted.

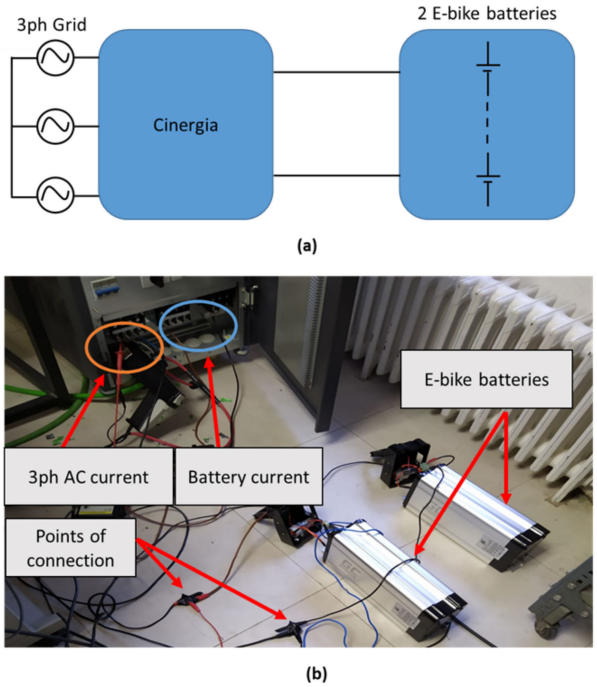

FIGURE 8. Experimental setup: (a) Electrical scheme; (b) Setup image.

TABLE 2. Main characteristics of the components and instruments in the experimental setup.

Device	Model	Specifications
Bidirectional Battery Charger.	B2C30.	DC part (independent mode): 750 Vmax (using 400 V), +-30 A.
E-BIKE Batteries.	GC E-BIKE Battery 48 V 20.4 Ah.	Electric Bicycle Bike Silverfish Li-Ion Battery
Oscilloscope.	ROHDE & SCHWARZ RTE 1104.	1 GHz, 5 GSa/s.
Differential (Voltage) probe.	TESTEC TT –SI 9010.	+-7 Kv at1/1000 or +-700 V at 1/100.
Current probes.	RT-ZC20B.	0.1 V/A, 100 MHz, 30 Arms.

The Cinergia converter is very flexible and it can work in different operating modes, but in this experiment is working as a current source following the battery current reference (I_{ref}). The DC output current of the Cinergia converter throughout the experiment is circulating through the 2 E-BIKE Batteries, which are connected in series. On the charging state, the maximum voltage that can be used is 50 V, while the current can reach up to 5 A. Both batteries are provided with a Battery Management System (BMS). The manufacturer provides some vague information about its topology, which is a back to back topology with active

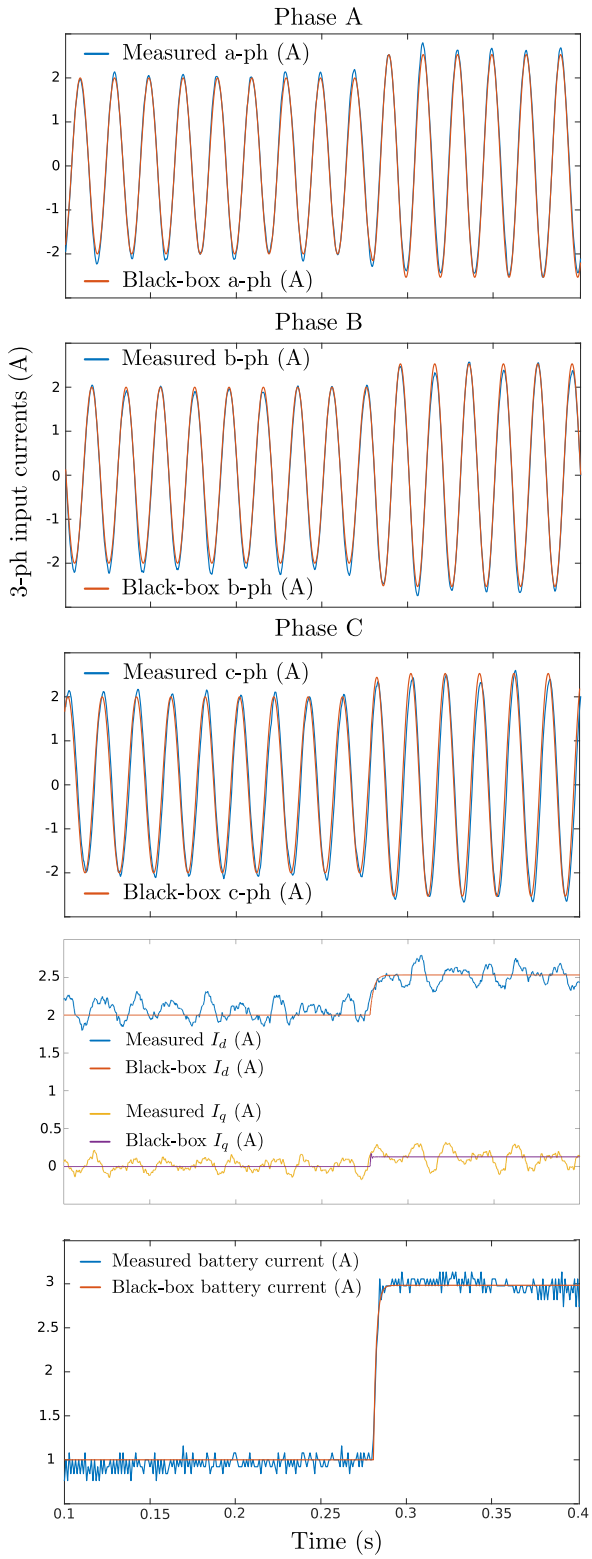

FIGURE 9. Comparison between the response of the actual charger and the small-signal black-box model for a 2 A step in the reference of charging current in G2V operation: 3-ph input currents, D-Q input currents, and battery current.

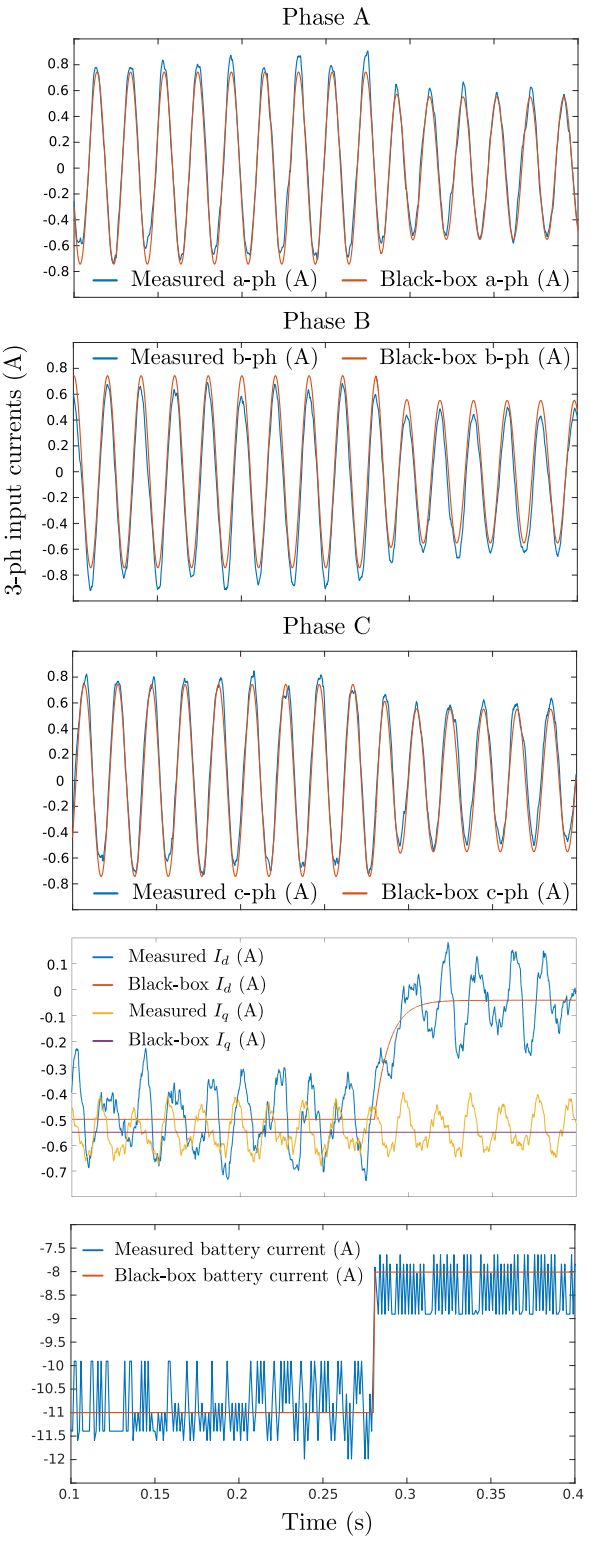

FIGURE 10. Comparison between the response of the actual charger and the small-signal black-box model for a 3A step in the reference of charging current in V2G operation: 3-ph input currents, D-Q input currents, and battery current.

rectification and a three-phase inverter using a proportional resonant controller [33].

The experiments in the current section are oriented to check the accuracy of the small-signal black-box models in three-phase battery chargers. The models should be able to

TABLE 3. Identified transfer functions from the experimental setup.

TF	G2V	V2G
$H_{dref}(s)$	$\frac{126.8}{s+480.3}$	$\frac{17.64}{s+115.3}$
$H_{qref}(s)$	$\frac{1.338e6}{s^2+2740s+2.124e7}$	$Neglected$
$H_{batref}(s)$	$\frac{574.5}{s+574.5}$	$\frac{7746}{s+7746}$

foresee the charger behavior through the estimation of the battery current and the three-phase AC input currents when small steps are given in the battery current reference. In the experimental setup the model is compared with the actual equipment. In this approach, the reference battery current is considered as the unique input variable to the model, assuming that the AC input voltage keeps constant. On the other hand, the battery current (I_{bat}) and the three-phase AC currents (I_{abc}) are the output variables to be estimated by the model.

In the first experiment, a step in the reference of battery current is applied. The battery current reference is increased from 1 A to 3 A at 0.28 s, working in G2V operation. In Fig. 9, it can be seen the comparison between the black-box model and the measurement from the actual equipment, where it is shown the AC input current, the d and q components of the input current, and the battery current. The model output is represented in orange colour and the actual measurements in blue colour. Again, the black-box AC input current is the result of the combination of the small-signal dynamic response of its d and q-components, the addition of the operating point, and the D-Q to ABC transformation (see Fig. 2). The D-Q framework has been set such that the q-component of the three-phase voltage is zero. It can be seen that it represents reasonably well the amplitude and phase of the three-phase AC input current of the battery charger.

The second experiment represents a discharge step in the battery. In order to discharge the battery, the polarity of the current induced is reversed. The battery current reference increases from -11 A to -8 A at 0.28 s. In Fig. 10, as in Fig. 9, it can be seen the comparison between the black-box model and the measurement from the actual equipment. The model output is also represented in orange colour and the actual measurements in blue colour. It can be seen how the Cinergia converter demands some reactive power, which remains constant, when working in V2G mode.

Looking at the waveforms in Fig. 9 and 10, it is quite easy to conclude the good accuracy of the black-box model in the tested conditions for three-phase battery chargers. However, it is highlighted that the battery charger has a different dynamic behavior depending on the direction of the power flow, it can be seen how the transient behavior of the converter is much faster in G2V mode than in V2G mode, and that it demands some reactive power when working in V2G mode. The most relevant reduced order transfer functions identified have been included in Table 3. The small-signal black-box model structure proposed is able to reproduce the dynamic behavior of the battery charger in both operating points under small-signal perturbations, however, a nonlinear black-box structure would be necessary to account for changes between G2V and V2G operation in this case.

V. CONCLUSION

The proliferation of electric vehicles will be associated with a huge increase in the number of battery chargers, which will manage the exchange of energy between the electric vehicles and the grid. The integration of a huge number of AC/DC converters in the power distribution system, especially in islanded systems, can have a negative influence in its dynamic behavior. Furthermore, the variety of commercial battery chargers, about which the information is very limited, make the system-level analysis of these architectures very difficult.

A possible solution is the use of black-box models, which can approximate the dynamic behavior of power electronic converters by analyzing the response of the output terminals of the devices to specific perturbances. The black-box approaches have been successfully applied to DC/DC converters and DC microgrids, however, the number of studies about AC/DC converters is very limited due to their complexity.

This work extends some of the black-box modeling techniques applied to DC/DC converters to single-phase and three-phase AC/DC converters, in particular to electric vehicle AC/DC battery chargers. The small-signal model is described, identifying the input and output variables and transforming AC signals in DC ones by means of the Park transformation. This model has been both mathematically defined and represented with an electrical equivalent model.

This approach has been validated by means of simulations and experimental tests. The obtained results show how the black-box small-signal model is able to approximate the dynamic behavior of single-phase and three-phase AC/DC battery chargers. It is true that the accuracy of the small-signal models is limited by the amplitude of the perturbations in the input variables. However, both through simulation and experiments, the proposed model shows a good accuracy in all conditions.

REFERENCES

[1] EVgo Services LLC. *BEVS, PHEVS AND HEVS, Which Electric Vehicle Do You Drive Types of Electric Vehicles*. Accessed: Jul. 30, 2020. [Online]. Available: https://www.evgo.com/why-evs/types-of-electric-vehicles/

[2] Electric Vehicle Basics. *Department of Energy. Office of Energy Efficiency & Renewable Energy*. Accessed: Jul. 30, 2020. [Online]. Available: https://www.energy.gov/eere/electricvehicles/electric-vehicle-basics

[3] Texas Instruments. (2018). *Taking Charge of Electric Vehicles—Both in the Vehicle and on the Grid*. [Online]. Available: http://www.ti.com/lit/wp/szzy007/szzy007.pdf

[4] B. Lunz and D. Sauer, "Electric road vehicle battery charging systems and infrastructure," in *Advances in Battery Technologies for Electric Vehicles*, B. Scrosati, J. Garche, and W. Tillmetz, Eds. Chicago, IN, USA: Woodhead, 2015, pp. 445–467. [Online]. Available: http://www.sciencedirect.com/science/article/pii/B9781782423775000170

[5] H. Liu, Y. Zhang, S. Zheng, and Y. Li, "Electric vehicle power trading mechanism based on blockchain and smart contract in V2G network," *IEEE Access*, vol. 7, pp. 160546–160558, 2019.

[6] A. Mehrabi, H. S. V. S. K. Nunna, A. Dadlani, S. Moon, and K. Kim, "Decentralized greedy-based algorithm for smart energy management in plug-in electric vehicle energy distribution systems," *IEEE Access*, vol. 8, p. 75666–75681, 2020.

[7] J. Balcells and J. Garcia, "Impact of plug-in electric vehicles on the supply grid," in *Proc. IEEE Vehicle Power Propuls. Conf.*, Sep. 2010, pp. 1–4.

[8] Autofutures. *How V2G Can Support the Grid and Help Pay Back Electric Vehicle Owners*. Accessed: Jul. 30, 2020. [Online]. Available: https://www.autofutures.tv/2019/09/02/v2g-can-help-support-the-grid/

[9] Smart Energy international. *The UK Pilots Smart EV Charging Hubs With V2G and Storage*. Accessed: Jul. 30, 2020. [Online]. Available: https://www.smart-energy.com/industry-sectors/electric-vehicles/the-uk-%pilots-smart-ev-charging-hubs-with-v2g-and-storage/

[10] The Mobility House. *Vehicle to Grid*. Accessed: Jul. 30, 2020. [Online]. Available: https://www.mobilityhouse.com/int_en/vehicle-to-grid

[11] S. Amamra and J. Marco, "Vehicle-to-grid aggregator to support power grid and reduce electric vehicle charging cost," *IEEE Access*, vol. 7, pp. 178528–178538, 2019.

[12] O. Kolawole and I. Al-Anbagi, "Electric vehicles battery wear cost optimization for frequency regulation support," *IEEE Access*, vol. 7, pp. 130388–130398, 2019.

[13] J. Sjöberg, Q. Zhang, L. Ljung, A. Benveniste, B. Delyon, P.-Y. Glorennec, H. Hjalmarsson, and A. Juditsky, "Nonlinear black-box modeling in system identification: A unified overview," *Automatica*, vol. 31, no. 12, pp. 1691–1724, Dec. 1995. [Online]. Available: http://www.sciencedirect.com/science/article/pii/0005109895001208

[14] L. Arnedo, R. Burgos, D. Boroyevich, and F. Wang, "System-level black-box DC-to-DC converter models," in *Proc. IEEE Appl. Power Electron. Conf. Expo.*, Feb. 2009, pp. 1476–1481.

[15] S. Vesti, J. A. Oliver, R. Prieto, J. A. Cobos, and T. Suntio, "Simplified small-signal stability analysis for optimized power system architecture," in *Proc. Annu. IEEE Appl. Power Electron. Conf. Expo. (APEC)*, 2013, pp. 1702–1708.

[16] V. Valdivia, A. Barrado, A. Lazaro, C. Fernandez, and P. Zumel, "Black-box modeling of DC-DC converters based on transient response analysis and parametric identification methods," in *Proc. IEEE Appl. Power Electron. Conf. Expo. (APEC)*, Feb. 2010, pp. 1131–1138.

[17] L. Arnedo, D. Boroyevich, R. Burgos, and F. Wang, "Un-terminated frequency response measurements and model order reduction for black-box terminal characterization models," in *Proc. IEEE Appl. Power Electron. Conf. Expo.*, Feb. 2008, pp. 1054–1060.

[18] I. Cvetkovic, D. Boroyevich, P. Mattavelli, F. C. Lee, and D. Dong, "Unterminated small-signal behavioral model of DC–DC converters," *IEEE Trans. Power Electron.*, vol. 28, no. 4, pp. 1870–1879, Apr. 2013.

[19] H. Gong, D. Yang, and X. Wang, "Identification of the DQ impedance model for three-phase power converter considering the coupling effect of the grid impedance," in *Proc. IEEE Appl. Power Electron. Conf. Expo. (APEC)*, Mar. 2019, pp. 120–126.

[20] V. Valdivia, A. Lazaro, A. Barrado, P. Zumel, C. Fernandez, and M. Sanz, "Black-box modeling of three-phase voltage source inverters for system-level analysis," *IEEE Trans. Ind. Electron.*, vol. 59, no. 9, pp. 3648–3662, Sep. 2012.

[21] G. Guarderas, A. Frances, R. Asensi, and J. Uceda, "Large-signal black-box behavioral modeling of grid-supporting power converters in AC microgrids," in *Proc. IEEE 6th Int. Conf. Renew. Energy Res. Appl. (ICRERA)*, Nov. 2017, pp. 153–158.

[22] H. Ali, H. Liu, X. Zheng, P. Gao, and H. Zaman, "Frequency response based behavioral modeling verification for three phase AC-DC converter," in *Proc. 43rd Annu. Conf. Ind. Electron. Soc.*, Oct. 2017, pp. 4908–4912.

[23] V. Ceperic, G. Gielen, and A. Baric, "Black-box modelling of AC-DC rectifiers for RFID applications using support vector regression machines," in *Proc. UKSim 15th Int. Conf. Comput. Modeling Simulation*, Apr. 2013, pp. 815–819.

[24] M. Veerachary and A. R. Saxena, "G-parameter based stability analysis of DC-DC power electronic system," in *Proc. Joint Int. Conf. Power Syst. Technol. IEEE Power India Conf.*, Oct. 2008, pp. 1–4.

[25] G. Guarderas, A. Frances, D. Ramirez, R. Asensi, and J. Uceda, "Blackbox large-signal modeling of grid-connected DC-AC electronic power converters," *Energies*, vol. 12, no. 6, p. 989, Mar. 2019, doi: 10.3390/en12060989.

[26] A. Frances, R. Asensi, O. Garcia, R. Prieto, and J. Uceda, "Modeling electronic power converters in smart DC microgrids—An overview," *IEEE Trans. Smart Grid*, vol. 9, no. 6, pp. 6274–6287, Nov. 2018.

[27] A. Frances-Roger, A. Anvari-Moghaddam, E. Rodriguez-Diaz, J. C. Vasquez, J. M. Guerrero, and J. Uceda, "Dynamic assessment of COTS converters-based DC integrated power systems in electric ships," *IEEE Trans. Ind. Informat.*, vol. 14, no. 12, pp. 5518–5529, Dec. 2018.

[28] D. Boroyevich, I. Cvetkovic, D. Dong, R. Burgos, F. Wang, and F. Lee, "Future electronic power distribution systems a contemplative view," in *Proc. 12th Int. Conf. Optim. Electr. Electron. Equip.*, May 2010, pp. 1369–1380.

[29] A. Francãs, R. Asensi, and J. Uceda, "Blackbox polytopic model with dynamic weighting functions for dc-dc converters," *IEEE Access*, vol. 7, pp. 160263–160273, 2019.

[30] H. Liu, Y. Tang, Y. Feng, and X. Ma, "A power quality disturbance classification method based on park transform and clarke transform analysis," in *Proc. 3rd Int. Conf. Innov. Comput. Inf. Control*, 2008, p. 524.

[31] C. J. O'Rourke, M. M. Qasim, M. R. Overlin, and J. L. Kirtley, "A geometric interpretation of reference frames and transformations: Dq0, clarke, and park," *IEEE Trans. Energy Convers.*, vol. 34, no. 4, pp. 2070–2083, Dec. 2019.

[32] A. Naziris, R. Asensi, and J. Uceda, "Black box modelling of a bidirectional battery charger for electric vehicles," in *Proc. 7th Int. Conf. Renew. Energy Res. Appl. (ICRERA)*, Oct. 2018, pp. 469–473.

[33] CINERGIA. (Sep. 2019). *Regenerative Power Electronics Solutions*. [Online]. Available: https://www.cinergia.coop/wp-content/uploads/2020/01/B2C-v6.1.pdf

ANTREAS NAZIRIS (Student Member, IEEE) was born in Nicosia, Cyprus, in 1988. He received the M.Eng. degree in electrical and electronic engineering from the University of Newcastle upon Tyne, in 2013. He is currently pursuing the Ph.D. degree with the Universidad Politécnica de Madrid. His research interests include smart grids and microgrids.

AIRAN FRANCES (Member, IEEE) received the M.Sc. and Ph.D. degrees in electrical engineering from the Universidad Politécnica de Madrid (UPM), Spain, in 2012 and 2018, respectively.

He is currently an Assistant Professor with the Department of Electrical Engineering, UPM. He participated for two years in the European Project XFEL, where he collaborated in the design and development of dc–dc power supplies for superconducting magnets. His current research interests include modeling, control and stability assessment of electronic power distribution systems, and smart grids.

RAFAEL ASENSI was born in Madrid, Spain, in 1966. He received the M.Sc. and Ph.D. degrees in electrical engineering from the Universidad Politécnica de Madrid (UPM), Madrid, Spain, in 1991 and 1998, respectively.

He joined the Department of Electrical Engineering, UPM, in 1994, where he is currently an Associate Professor. His research interests include high-frequency modeling of magnetic components and non-linear load modeling and simulation.

JAVIER UCEDA (Life Fellow, IEEE) received the M.Sc. and Ph.D. degrees in electrical engineering from the Universidad Politécnica de Madrid (UPM), Spain, in 1976 and 1979, respectively.

He is currently a Full Professor of electronics with the Electrical and Electronic Engineering Department, UPM. His research activity has been developed in the field of power electronics, where he has participated in numerous national and international research projects. As a result of this activity he has published more than three hundred articles in international journals and conferences. He holds several national and international patents. His research interests include switched-mode power supplies and dc–dc power converters for telecom and aerospace applications.

Dr. Uceda has received several individual and collective awards, such as the IEEE Third Millennium Medal and the Puig Adam Medal. He is also an Honorary Doctor by the Universidad Ricardo Palma in Peru and the Colegio de Posgraduados in Mexico.